JOURNAL OF SOLID STATE CHEMISTRY 92, 261–272 (1991)

Synthesis and Structure Refinement of $SrT_xV_{6-x}O_{11}$ (T = Ti, Cr, and Fe)

Y. KANKE,* F. IZUMI, E. TAKAYAMA-MUROMACHI, AND K. KATO

National Institute for Research in Inorganic Materials, 1-1 Namiki, Tsukuba, Ibaraki 305, Japan

AND T. KAMIYAMA AND H. ASANO

Institute of Material Science, University of Tsukuba, Tennodai, Tsukuba, Ibaraki 305, Japan

Received August 13, 1990; in revised form January 8, 1991

Four new phases, SrV_6O_{11}, $SrTi_xV_{6-x}O_{11}$ ($0 < x \leq 1.5$), $SrCr_xV_{6-x}O_{11}$ ($0 < x \leq 1.0$), and $SrFe_xV_{6-x}O_{11}$ ($0 < x \leq 1.4$), were synthesized. All of them have hexagonal symmetry (space group: $P6_3/mmc$) and are isostructural with NaV_6O_{11}, $BaTi_2Fe_4O_{11}$, and $BaSn_2Fe_4O_{11}$. The structures of $SrTiV_5O_{11}$, $SrTi_{1.5}V_{4.5}O_{11}$, $SrCrV_5O_{11}$, and $SrFeV_5O_{11}$ were refined by Rietveld analysis of their neutron powder diffraction data. Some structural features of these four compounds are discussed in comparison with those of SrV_6O_{11}, $BaTi_2Fe_4O_{11}$, and $BaSn_2Fe_4O_{11}$.

Introduction

De Roy *et al.* (*1*) synthesized NaV_6O_{11} for the first time by electrolytic reduction of molten $NaVO_3$. In the course of a phase equilibrium study on a NaV_2O_5–V_2O_3–V_2O_5 system (*2*), we also obtained NaV_6O_{11} by solid state reaction. Our literature survey (*3*) revealed that NaV_6O_{11} (hexagonal, $P6_3/mmc$) is essentially isostructural with $BaTi_2Fe_4O_{11}$ and $BaSn_2Fe_4O_{11}$ (*4*) (AT_6O_{11}-type compounds: A, alkaline metals or alkaline earth metals; T, transition metals), which are structurally related to $BaFe_{12}O_{19}$ (*5*). Figure 1 shows the stacking sequences of layers along c-axes in $BaFe_{12}O_{19}$ and AT_6O_{11}-type compounds. In $BaFe_{12}O_{19}$, Fe(1) and Fe(5) octahedra and Fe(3) tetrahedra form spinel-blocks (S), while Fe(2), Fe(4), and Fe(5) polyhedra construct so-called R-blocks (R) (*6*). The AT_6O_{11}-type compounds consist exclusively of R-blocks. The unit cell of $BaFe_{12}O_{19}$ can be expressed as $(RS)_2$, and that of the AT_6O_{11}-type compounds as R_2.

The R-block contains two octahedral sites: $M(1)$ and $M(2)$ in AT_6O_{11}, and the corresponding Fe(5) and Fe(4) in $BaFe_{12}O_{19}$. The $M(1)O_6$ octahedra are connected by edge sharing to form an $[M(1)O_6]_\infty$ sheet perpendicular to the c-axis. Two $M(2)$ atoms neighbor closely across a mirror plane ($M(3)$ plane) perpendicular to the c-axis, sharing an octahedral face. $M(3)$ in the mirror plane ($2d$ position, (1/3, 2/3, 3/4)) is a trigonal–bipyramidal site. This site is, however, usu-

* To whom correspondence should be addressed.

0022-4596/91 $3.00

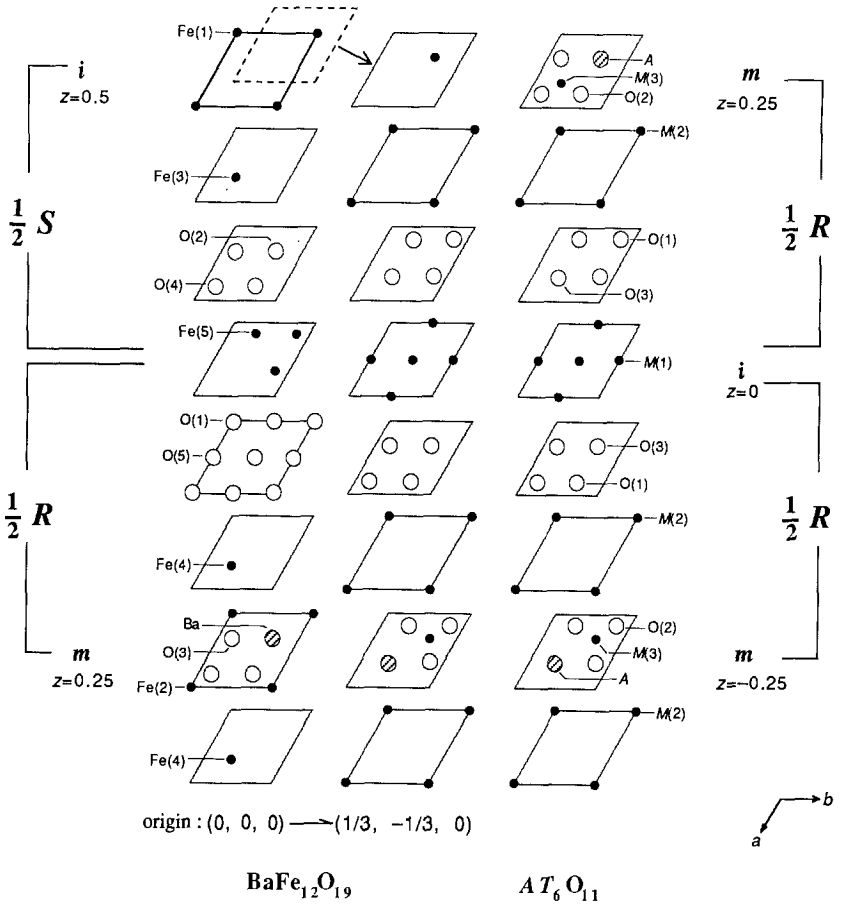

FIG. 1. Stacking sequences of layers along the c-axis in $BaFe_{12}O_{19}$ (left and middle layers) and AT_6O_{11} (right layers). Atoms are shown layer by layer parallel to [001]. The origin in $BaFe_{12}O_{19}$ is shifted from (0, 0, 0) in the left layers to (1/3, −1/3, 0) in the middle layers. The mirror planes (m) are at $z = 0.25$ and 0.75. The centers of symmetry (i) are at (1/2, 1/2, 0) and (1/2, 1/2, 1/2) in both of the two structures. S represents the spinel-block, and R indicates the so-called R-block.

ally split along the c-axis into a pair of distorted tetrahedral sites (4f position, (1/3, 2/3, 3/4 ± Δz)) and a T atom occupies one of the paired positions arbitrarily, except for the case of NaV_6O_{11}. In the AT_6O_{11}-type compounds, half of T atoms occupy the $M(1)$ site, one-third of them are placed in the $M(2)$ site, and the remaining one-sixth of them occupy the $M(3)$ site.

In $BaFe_{12}O_{19}$, all Fe atoms are trivalent. In the AT_6O_{11}-type compounds, on the other hand, both trivalent and tetravalent metals are contained as T, and their ratio depends on the valence of the A atom. The T^{3+}/T^{4+} ratio is 4/2 in both $BaTi_2Fe_4O_{11}$ and $BaSn_2Fe_4O_{11}$ while it is 3/3 in NaV_6O_{11}. A neutron powder diffraction study (*4*) indicated that the $M(3)$ sites of $BaTi_2Fe_4O_{11}$ and $BaSn_2Fe_4O_{11}$ are occupied by Fe^{3+} exclusively. This site-occupation behavior is consistent with the results of Madelung energy calculations (*3*), which indicate that both $BaTi_2Fe_4O_{11}$ and $BaSn_2Fe_4O_{11}$ are electrostatically most stable when $M(1)$, $M(2)$, and $M(3)$ sites are occupied by trivalent, tetravalent, and trivalent cations, respectively. On the

contrary, NaV_6O_{11} is electrostatically most stable when $M(1)$, $M(2)$, and $M(3)$ sites are occupied by V^{3+}, V^{4+}, and V^{4+}, respectively (*3*).

Resistivities of NaV_6O_{11} perpendicular to [001] show an anomaly at around 64 K. Preliminary experiments indicated that there is a magnetic transition at around 60 K, corresponding to the anomaly in resistivity (*2*). $BaTi_2Fe_4O_{11}$ was reported to show ferrimagnetic behavior with a Néel temperature between 120 and 200 K (*7*), though its magnetic structure has not been revealed yet. $BaFe_{12}O_{19}$ shows ferrimagnetic behavior with a Néel temperature of 723 K (*8*), and its magnetic structure has been analyzed in Mössbauer (*9*) and ESR (*10*) studies.

We have been trying to substitute the Na and V atoms in NaV_6O_{11} and found four new phases, SrV_6O_{11}, $SrTi_xV_{6-x}O_{11}$ ($0 < x \leq 1.5$), $SrCr_xV_{6-x}O_{11}$ ($0 < x \leq 1.0$), and $SrFe_xV_{6-x}O_{11}$ ($0 < x \leq 1.4$). The structure of SrV_6O_{11} has already been refined by X-ray diffraction using a single crystal (*3*). In the present study, the structures of $SrTiV_5O_{11}$, $SrTi_{1.5}V_{4.5}O_{11}$, $SrCrV_5O_{11}$, and $SrFeV_5O_{11}$ were refined by Rietveld analysis of their neutron powder diffraction data. Their diffraction patterns had somewhat low S/N ratios because V scatters neutrons almost incoherently. However, the present refinements were successful, as described below. Ti, Cr, and Fe could be easily distinguished from V because the absolute value of the coherent scattering length for V is much smaller than those of the other three metals.

Synthesis

V_2O_3 was prepared by reducing V_2O_5 (99.9%) in hydrogen at 1073 K. $Sr_2V_2O_7$ was obtained by heating a mixture of $SrCO_3$ (99.9%) and V_2O_5 in a 2 : 1 molar ratio at 1173 K for 5 days. $SrTiO_3$ was prepared by heating an equimolar mixture of $SrCO_3$ and TiO_2 (rutile, reagent grade) at 1373 K for 5 days.

SrV_6O_{11} was prepared by solid state reaction using $Sr_2V_2O_7$ and V_2O_3 as starting reagents. $Sr_2V_2O_7$ and V_2O_3 were mixed in a 1 : 5 molar ratio. About 1.5 g of the mixture was placed in a platinum capsule, sealed in an evacuated silica tube, and then heated at 1473 K for 1 day. After having cooled to room temperature, the product was ground and identified by X-ray powder diffraction with Cu$K\alpha$ radiation. This procedure was repeated until its X-ray powder pattern changed no longer. One heating run was enough to reach equilibrium.

$SrCr_xV_{6-x}O_{11}$ samples were prepared in the same manner from starting compounds, $Sr_2V_2O_7$, Cr_2O_3 (99.9%), and V_2O_3. Besides the 1.5-g batch, a sample for neutron diffraction was prepared as a separate 10-g batch. The number of heating cycles necessary to reach equilibrium was one in the 1.5-g batch and two in the 10-g batch. A sample with $x = 1.0$ was a single phase, whereas another one with $x = 1.1$ was not. Thus the x range in $SrCr_xV_{6-x}O_{11}$ is $0 < x \leq 1.0$ at 1473 K.

$SrFe_xV_{6-x}O_{11}$ samples were prepared in the same way from starting compounds, $Sr_2V_2O_7$, Fe_2O_3 (99.9%), and V_2O_3. Equilibrium was attained in one heating cycle for both 1.5-g and 10-g batches. The x range ($0 < x \leq 1.0$) at 1473 K was determined by the above method. The x range became wider at 1273 K ($0 < x \leq 1.4$). $SrFe_xV_{6-x}O_{11}$ with $x > 1$ decomposed at 1473 K.

$SrTi_xV_{6-x}O_{11}$ samples were synthesized in the same manner from $Sr_2V_2O_7$, $SrTiO_3$, TiO_2, and V_2O_3. Two or three heating cycles were needed for both 1.5-g and 10-g batches to reach equilibrium. The x range ($0 < x \leq 1.5$) at 1473 K was determined by the above method. A sample of $SrTi_{1.5}V_{4.5}O_{11}$ for a neutron diffraction experiment, however, proved to contain small amounts of impurities, $SrTiO_3$, and unknown substances. It seems difficult to synthesize a large amount of pure $SrTi_{1.5}V_{4.5}O_{11}$ in one batch.

The X-ray powder diffraction patterns of SrV_6O_{11}, $SrTiV_5O_{11}$, $SrCrV_5O_{11}$, and $SrFeV_5O_{11}$ (Tables I–IV) indicate that the

TABLE I

X-RAY POWDER PATTERN OF SrV_6O_{11}

h	k	l	d_{obs}(Å)	d_{calc}(Å)	I/I_0	h	k	l	d_{obs}(Å)	d_{calc}(Å)	I/I_0
0	0	2	6.529	6.545	1	4	0	2	1.2272	1.2272	2
1	0	1	4.664	4.669	2	4	0	3	1.2010	1.2011	1
1	0	2	3.972	3.972	5	1	1	10	1.1922	1.1921	7
0	0	4	3.2709	3.2727	36	3	1	6	1.1701	1.1699	1
1	1	0	2.8840	2.8853	30	3	0	8	1.1674	1.1673	2
1	0	4	2.7372	2.7378	100	2	0	10	1.1595	1.1596	1
1	1	2	2.6396	2.6401	66	2	1	9	1.1524	1.1524	<1
2	0	0	2.4978	2.4987	5	3	2	2	1.1290	1.1293	<1
2	0	2	2.3337	2.3344	35	0	0	12	1.0913	1.0909	3
1	0	5	2.3182	2.3191	2	4	0	6	1.0843	1.0842	6
0	0	6	2.1820	2.1818	4	2	2	8	1.0823	1.0821	8
2	0	3	2.1681	2.1684	33	3	2	4	1.0819	1.0820	7
1	0	6	1.9995	1.9995	7	4	1	2	1.0756	1.0757	4
2	0	5	1.8072	1.8076	<1	3	1	8	1.0577	1.0576	<1
1	0	7	1.7523	1.7515	1	3	0	10	1.0290	1.0293	3
1	1	6	1.7400	1.7402	5	1	1	12	1.0205	1.0204	<1
2	1	3	1.7330	1.7334	1	3	2	6	1.0149	1.0149	<1
3	0	0	1.6656	1.6658	4	2	1	11	1.0068	1.0069	<1
2	0	6	1.6434	1.6435	57	4	1	5	1.0068	1.0067	<1
0	0	8	1.6360	1.6363	40	5	0	0	0.9992	0.9995	<1
2	1	4	1.6360	1.6359	40	4	0	8	0.9930	0.9930	1
3	0	2	1.6140	1.6143	10	5	0	2	0.9878	0.9880	<1
1	0	8	1.5548	1.5551	2	3	2	7	0.9777	0.9774	<1
2	1	5	1.5318	1.5318	1	4	1	6	0.9755	0.9755	1
2	0	7	1.4979	1.4972	<1	2	2	10	0.9695	0.9694	<1
2	2	0	1.4426	1.4426	18	5	0	4	0.9559	0.9559	1
2	1	6	1.4281	1.4280	3	3	3	2	0.9516	0.9515	1
1	1	8	1.4232	1.4234	4	4	0	9	0.9477	0.9477	1
2	0	8	1.3685	1.3689	31	2	1	12	0.9445	0.9447	1
3	0	6	1.3239	1.3240	1	4	2	2	0.9348	0.9347	1
2	2	4	1.3202	1.3201	4	4	2	3	0.9233	0.9231	1
3	1	4	1.2763	1.2763	6	3	0	12	0.9124	0.9126	<1
1	0	0	1.2666	1.2663	2	4	1	8	0.9075	0.9075	1
2	0	9	1.2572	1.2571	3	4	0	10	0.9038	0.9038	<1
2	1	8	1.2365	1.2368	1						

four new phases are isostructural with NaV_6O_{11}. Their lattice parameters determined by X-ray powder diffraction are given in Table V. Figure 2 shows the lattice parameters of the $SrT_xV_{6-x}O_{11}$ phases as functions of x.

Among various divalent or trivalent metals such as Ca, Sr, Ba, La, and Nd, only Sr was acceptable as A in AT_6O_{11}-type compounds at 1473 K.

Neutron Diffraction Experiments and Structure Refinements

Neutron diffraction data of $SrTiV_5O_{11}$, $SrTi_{1.5}V_{4.5}O_{11}$, $SrCrV_5O_{11}$, and $SrFeV_5O_{11}$ were taken on a time-of-flight (TOF) neutron powder diffractometer, HRP (*11*), at the KENS pulsed spallation neutron source of the National Laboratory for High Energy Physics. The sample was contained in a cy-

TABLE II

X-RAY POWDER PATTERN OF $SrTiV_5O_{11}$

h	k	l	d_{obs}(Å)	d_{calc}(Å)	I/I_0	h	k	l	d_{obs}(Å)	d_{calc}(Å)	I/I_0
1	0	1	4.678	4.684	3	3	0	8	1.1739	1.1741	2
1	0	2	3.987	3.991	5	2	0	10	1.1683	1.1684	2
0	0	4	3.3012	3.3023	34	2	1	9	1.1600	1.1600	<1
1	1	0	2.8909	2.8922	34	3	2	2	1.1321	1.1322	<1
1	0	4	2.7569	2.7571	100	0	0	12	1.1007	1.1008	3
1	1	2	2.6488	2.6493	72	4	1	0	1.0932	1.0932	2
2	0	0	2.5047	2.5047	6	4	0	6	1.0884	1.0886	10
2	0	2	2.3421	2.3420	41	2	2	8	1.0878	1.0879	9
0	0	6	2.2020	2.2016	3	3	2	4	1.0854	1.0854	4
2	0	3	2.1767	2.1771	36	2	1	10	1.0831	1.0833	1
1	0	6	2.0157	2.0155	7	2	0	11	1.0831	1.0828	1
1	1	6	1.7519	1.7518	5	4	1	2	1.0784	1.0785	3
3	0	0	1.6700	1.6698	4	1	0	12	1.0750	1.0751	1
2	0	6	1.6536	1.6536	66	3	1	8	1.0631	1.0631	<1
2	1	4	1.6425	1.6426	31	3	0	10	1.0360	1.0360	4
3	0	2	1.6189	1.6189	13	1	1	12	1.0286	1.0288	<1
1	0	8	1.5681	1.5682	1	3	2	6	1.0187	1.0188	1
2	0	7	1.5068	1.5072	<1	2	1	11	1.0138	1.0141	1
2	2	0	1.4461	1.4461	21	4	0	8	0.9977	0.9978	1
2	1	6	1.4353	1.4355	5	4	1	6	0.9790	0.9791	1
1	1	8	1.4337	1.4339	5	2	2	10	0.9753	0.9753	<1
1	0	9	1.4090	1.4085	<1	3	3	0	0.9642	0.9641	1
2	0	8	1.3785	1.3786	5	5	0	4	0.9588	0.9587	2
3	0	6	1.3302	1.3304	2	3	1	10	0.9572	0.9573	1
2	2	4	1.3245	1.3247	4	3	3	2	0.9540	0.9540	1
3	1	4	1.2805	1.2807	7	4	0	9	0.9528	0.9527	1
1	0	10	1.2772	1.2773	2	2	1	12	0.9516	0.9516	1
2	0	9	1.2661	1.2663	4	4	2	0	0.9467	0.9467	<1
4	0	0	1.2524	1.2524	1	0	0	14	0.9435	0.9435	<1
2	1	8	1.2442	1.2444	2	4	2	2	0.9371	0.9371	1
4	0	2	1.2303	1.2305	3	1	0	14	0.9273	0.9272	1
4	0	3	1.2045	1.2046	2	4	2	3	0.9255	0.9256	1
1	1	10	1.2015	1.2015	8	4	1	8	0.9115	0.9115	1
3	1	6	1.1750	1.1750	2	4	0	10	0.9090	0.9088	1

lindrical vanadium cell 5 mm in radius, 42 mm in height, and 25 μm in thickness and placed in an aluminum vacuum chamber. The cell was turned round on its axis during data collection. Intensity data were obtained at room temperature using twelve ^{3}He counters installed with an average 2θ of 170° and then time-focused by off-line data processing. The dependence of the incident intensity on TOF, t, was monitored during the data collection with a fission chamber. This spectrum was smoothed by the combination of Fourier transform, low-pass filtering, and inverse Fourier transform.

The resulting intensity data were analyzed by the Rietveld method with RIETAN (*12*). The coherent scattering lengths, b, used for refinements were 7.02 fm (Sr), −0.3824 fm (V), 3.635 fm (Cr), 9.54 fm (Fe), 5.803 fm (O) (*13*), and −3.438 fm (Ti) (*14*). Intensity data corresponding to interplanar spacings, d, between 0.506 and 3.296 Å

TABLE III

X-RAY POWDER PATTERN OF $SrCrV_5O_{11}$

h	k	l	d_{obs}(Å)	d_{calc}(Å)	I/I_0	h	k	l	d_{obs}(Å)	d_{calc}(Å)	I/I_0
1	0	1	4.670	4.667	2	4	0	2	1.2272	1.2271	2
1	0	2	3.968	3.968	5	4	0	3	1.2005	1.2008	1
0	0	4	3.2647	3.2643	51	1	1	10	1.1899	1.1896	7
1	1	0	2.8847	2.8852	25	3	1	6	1.1689	1.1690	1
1	0	4	2.7329	2.7329	100	3	0	8	1.1657	1.1658	2
1	1	2	2.6388	2.6390	58	2	0	10	1.1575	1.1572	1
2	0	0	2.4988	2.4987	5	0	0	12	1.0879	1.0881	3
2	0	2	2.3338	2.3336	28	4	0	6	1.0835	1.0835	5
1	0	5	2.3138	2.3145	2	2	2	8	1.0810	1.0809	6
0	0	6	2.1782	2.1762	5	4	1	2	1.0757	1.0756	2
2	0	3	2.1668	2.1670	27	1	0	12	1.0628	1.0632	1
1	0	6	1.9946	1.9952	6	3	1	8	1.0567	1.0565	<1
1	1	6	1.7378	1.7374	5	3	0	10	1.0276	1.0276	3
3	0	0	1.6663	1.6658	3	1	1	12	1.0182	1.0181	<1
2	0	6	1.6414	1.6411	51	3	2	6	1.0142	1.0143	<1
2	1	4	1.6347	1.6349	34	4	0	8	0.9922	0.9921	1
3	0	2	1.6139	1.6141	9	4	1	6	0.9750	0.9749	1
1	0	8	1.5517	1.5515	2	2	2	10	0.9679	0.9681	<1
2	2	0	1.4426	1.4426	15	5	0	4	0.9557	0.9557	1
2	1	6	1.4266	1.4265	3	3	1	10	0.9505	0.9504	1
1	1	8	1.4206	1.4206	4	4	0	9	0.9467	0.9467	1
2	0	8	1.3664	1.3665	4	2	1	12	0.9428	0.9429	1
2	2	4	1.3193	1.3195	3	4	2	2	0.9346	0.9347	1
3	1	4	1.2759	1.2758	6	4	2	3	0.9229	0.9229	1
1	0	10	1.2632	1.2633	2	4	1	8	0.9068	0.9067	1
2	0	9	1.2544	1.2547	3	4	0	10	0.9026	0.9027	<1
3	0	7	1.2424	1.2425	<1						
2	1	8	1.2349	1.2350	1						

were used for the Rietveld refinements, but those in the t regions 20,919–21,249, 21,279–21,299, 22,565–22,740, 23,859–24,009, 24,139–24,249, and 24,379–24,559 μs were excluded for $SrTi_{1.5}V_{4.5}O_{11}$ due to the appearance of weak peaks assigned to unknown impurities. A reflection was regarded as contributing to a profile up to a point for which (intensity of the reflection at the point)/(peak height) was 0.0025.

Rietveld refinements were started using the following crystallographic information: space group $P6_3/mmc$, lattice parameters determined by X-ray powder diffraction (Table V), atomic coordinates of NaV_6O_{11} (*3*). The occupation factors, g, of T atoms at the $M(1)$, $M(2)$, and $M(3)$ sites were varied during initial stages.

(*a*) *$SrFeV_5O_{11}$*. Although its structure parameters converged smoothly, the occupancy of Fe at the $M(1)$ site, g(Fe(1)), converged to a negative value, $-0.008(6)$. Subsequent refinement was carried out by fixing g(Fe(1)) at zero and giving anisotropic thermal parameters, U_{ii}, for the $M(3)$ site. The resulting ratio U_{33}/U_{11} was unreasonably large (0.114(7) Å^2/0.016(2) Å^2), suggesting a displacement of the $M(3)$ site from the ideal 2*d* position (1/3, 2/3, 3/4) to a pair of 4*f* positions (1/3, 2/3, 3/4 $\pm$ Δz). The following two structure models were tested:

TABLE IV

X-RAY POWDER PATTERN OF $SrFeV_5O_{11}$

h	k	l	d_{obs}(Å)	d_{calc}(Å)	I/I_0	h	k	l	d_{obs}(Å)	d_{calc}(Å)	I/I_0
0	0	2	6.602	6.611	2	2	1	8	1.2421	1.2424	<1
1	0	1	4.672	4.664	<1	4	0	2	1.2251	1.2246	<1
1	0	2	3.981	3.980	1	1	1	10	1.2015	1.2014	3
0	0	4	3.3045	3.3053	100	3	0	8	1.1715	1.1717	1
1	1	0	2.8784	2.8778	5	2	0	10	1.1679	1.1680	1
1	0	4	2.7548	2.7547	34	2	1	9	1.1587	1.1585	<1
1	1	2	2.6397	2.6386	14	0	0	12	1.1020	1.1018	4
2	0	0	2.4934	2.4923	1	3	0	9	1.1004	1.1006	2
2	0	2	2.3326	2.3321	7	4	1	0	1.0880	1.0877	<1
0	0	6	2.2030	2.2036	5	2	2	8	1.0850	1.0852	3
2	0	3	2.1697	2.1694	10	2	1	10	1.0820	1.0822	1
1	0	6	2.0152	2.0154	3	3	2	4	1.0806	1.0807	1
1	0	7	1.7661	1.7662	<1	1	0	12	1.0757	1.0758	1
1	1	6	1.7494	1.7496	1	4	1	2	1.0735	1.0733	1
3	0	0	1.6621	1.6615	1	3	1	8	1.0604	1.0604	<1
0	0	8	1.6528	1.6527	21	3	0	10	1.0345	1.0346	1
2	0	6	1.6506	1.6508	23	1	1	12	1.0288	1.0290	<1
2	1	4	1.6372	1.6368	7	3	2	6	1.0150	1.0150	<1
3	0	2	1.6117	1.6114	2	3	1	9	1.0066	1.0068	<1
1	0	8	1.5692	1.5687	1	4	0	8	0.9951	0.9950	<1
2	1	5	1.5335	1.5344	<1	4	1	6	0.9753	0.9754	<1
2	0	7	1.5060	1.5053	<1	2	2	10	0.9735	0.9736	<1
2	2	0	1.4394	1.4389	3	3	1	10	0.9554	0.9555	<1
1	1	8	1.4337	1.4332	1	4	0	9	0.9501	0.9503	<1
1	0	9	1.4090	1.4091	<1	0	0	14	0.9445	0.9444	<1
2	0	8	1.3775	1.3774	1	4	2	2	0.9327	0.9326	<1
3	0	6	1.3266	1.3267	<1	1	0	14	0.9279	0.9279	<1
2	2	4	1.3194	1.3193	1	4	2	3	0.9213	0.9212	<1
1	0	10	1.2783	1.2779	1	4	1	8	0.9084	0.9086	<1
3	1	4	1.2756	1.2754	2	4	0	10	0.9068	0.9068	<1
2	0	9	1.2656	1.2656	1						

(i) both of the Fe(3) and V(3) atoms at the 4*f* position and (ii) the Fe(3) atom at the 4*f* position and the V(3) atom at the ideal 2*d* position. In both of the refinements, the isotropic thermal parameters of V(3) and Fe(3) were constrained to be equal. The two refinements gave essentially the same *R* factors and structure parameters except for the *z* coordinates of V(3). Although there was no experimental evidence, we preferred the latter model because of reasons described later. The final parameters are presented in Table VI; lattice parameters, occupation factors, and interatomic distances in Table VII.

(*b*) $SrCrV_5O_{11}$. Because some variable parameters did not converge, we imposed additional constraints that the isotropic thermal parameters of the $M(1)$, $M(2)$, and $M(3)$ sites were all equal. The $M(3)$ cations were located at the 2*d* position because Cr^{3+}, V^{3+}, and V^{4+} generally do not take fourfold coordination. The refined parameters and interatomic distances are presented in Tables VI and VII, respectively. Figure 3 illustrates the final profile fit and difference pat-

TABLE V

LATTICE PARAMETERS OF THE NEW COMPOUNDS DETERMINED BY X-RAY POWDER DIFFRACTION

Compound	a (Å)	c (Å)
SrV_6O_{11}	5.7705(3)	13.0907(9)
$SrTiV_5O_{11}$	5.7845(2)	13.2093(9)
$SrCrV_5O_{11}$	5.7704(2)	13.0573(7)
$SrFeV_5O_{11}$	5.7557(4)	13.2213(9)

Note. In all tables, numbers in parentheses are estimated standard deviations of the last significant digit.

terns of $SrCrV_5O_{11}$ plotted against the scattering vector Q ($=2\pi/d$).

(*c*) *$SrTiV_5O_{11}$ and $SrTi_{1.5}V_{4.5}O_{11}$.* The parameters of $SrTiV_5O_{11}$ converged smoothly to final values without imposing further constraints. As described above, the $SrTi_{1.5}V_{4.5}O_{11}$ sample contained small amounts of $SrTiO_3$ and the unknown substances. Then, the structure parameters of $SrTi_{1.5}V_{4.5}O_{11}$ were refined by excluding the unknown impurity peaks and regarding the sample as a mixture of $SrTi_{1.5}V_{4.5}O_{11}$ and $SrTiO_3$ (*15*). Isotropic thermal parameters of the $M(1)$, $M(2)$, and $M(3)$ sites converged to values smaller than 0.1 Å^2 when they were varied. Therefore, these three parameters were fixed at 0.2 Å^2, which is an average of corresponding parameters for the three cation sites in $SrTiV_5O_{11}$. We could not conclude whether the $M(3)$ sites of $SrTiV_5O_{11}$ and $SrTi_{1.5}V_{4.5}O_{11}$ are at the ideal 2*d* positions or at the 4*f* positions. The influences of $SrTiO_3$ and the unknown impurities on final structure parameters seems to be negligible. That is, a single-phase refinement

TABLE VI

STRUCTURAL PARAMETERS IN $SrT_xV_{6-x}O_{11}$ COMPOUNDS

Atom	Parameter	$SrTiV_5O_{11}$	$SrTi_{1.5}V_{4.5}O_{11}$	$SrCrV_5O_{11}$	$SrFeV_5O_{11}$
$M(1)$	B (Å^2)	0.2(2)	0.2	1.3(4)	1.1(5)
$M(2)$	z	0.144(1)	0.145(1)	0.144(4)	0.1399(8)
$M(2)$	B (Å^2)	0.2(2)	0.2	1.3(4)	0.9(1)
$M(3)$	z	3/4	3/4	3/4	3/4[a] 0.7678(6)[b]
$M(3)$	B (Å^2)	0.2(3)	0.2	1.3(4)	1.8(2)
O(1)	x	0.1736(3)	0.1726(5)	0.1737(4)	0.1729(3)
O(1)	z	0.0826(2)	0.0813(4)	0.0815(3)	0.0841(2)
O(1)	B (Å^2)	0.42(3)	0.53(6)	0.69(5)	0.51(3)
O(2)	x	0.1529(4)	0.1523(6)	0.1546(4)	0.1527(3)
O(2)	B (Å^2)	0.57(4)	0.48(8)	0.30(4)	0.40(4)
O(3)	z	0.5903(3)	0.5894(6)	0.5914(3)	0.5909(3)
O(3)	B (Å^2)	0.75(7)	0.76(11)	0.67(7)	0.68(7)
Sr	B (Å^2)	1.4(1)	1.2(2)	0.39(8)	0.84(9)
	R_{wp}(%)	5.30	5.55	5.07	4.41
	R_p(%)	4.22	4.14	3.82	3.48
	R_I(%)	3.16	3.50	2.64	2.81

Note. For all compounds, $M(1)$: 6*g* position, $x = 1/2$, $y = 0$, $z = 0$. $M(2)$: 4*e* position, $x = 0$, $y = 0$. $M(3)$: 2*d* position except for $SrFeV_5O_{11}$, $x = 1/3$, $y = 2/3$. O(1): 12*k* position, $y = 2x$. O(2): 6*h* position, $y = 2x$, $z = 3/4$. O(3): 4*f* position, $x = 1/3$, $y = 2/3$. Sr: 2*c* position, $x = 1/3$, $y = 2/3$, $z = 1/4$. B is the isotropic thermal parameter. As described in the text, Bs of all the $M(n)$ sites for $SrCrV_5O_{11}$ were constrained to be equal, and those of $SrTi_{1.5}V_{4.5}O_{11}$ were fixed at 0.2 Å^2.

[a] V atom (2*d* position). B was constrained to be equal to that of the Fe(3) atom.

[b] Fe atom (4*f* position).

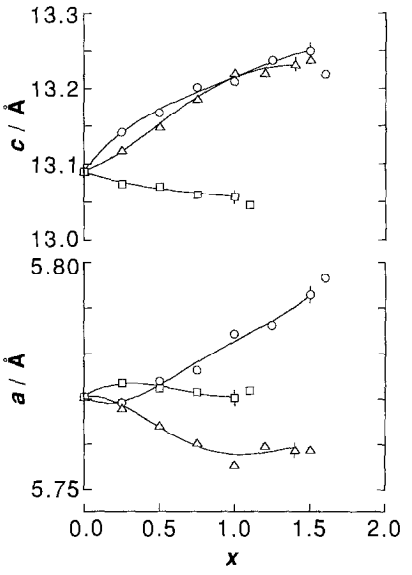

FIG. 2. Lattice parameters versus x for the systems $SrTi_xV_{6-x}O_{11}$ (○), $SrCr_xV_{6-x}O_{11}$ (□), and $SrFe_xV_{6-x}O_{11}$ (Δ). All samples were sintered at 1473 K except for $SrFe_{1.2}V_{4.8}O_{11}$, $SrFe_{1.4}V_{4.6}O_{11}$, and $SrFe_{1.5}V_{4.5}O_{11}$ (1273 K).

where the impurity peaks were included gave still low R factors (R_{wp} = 7.93%, R_p = 5.29%, and R_I = 5.76%) and the same structure parameters within standard deviations (e.g., g(Ti(1)) = 0.09(4), g(Ti(2)) = 0.43(6), and g(Ti(3)) = 0.38(18)) except for some refinable thermal parameters. The structure parameters and interatomic distances obtained in this way are presented in Tables VI and VII, respectively.

Discussion

(*a*) *$SrFeV_5O_{11}$*. The $M(3)$ site in this structure is 56% occupied by Fe ions and 44% by V ions. The V(3) atom is located at the ideal 2*d* position whereas the Fe(3) atom occupies either one of the adjacent 4*f* positions, (1/3, 2/3, 3/4 ± Δz) with Δz = 0.0178(6). This is in harmony with the fact that the V(3) sites in both SrV_6O_{11} and NaV_6O_{11} (*3*) are not split while the corresponding Fe ions in $BaTi_2Fe_4O_{11}$ and $BaSn_2Fe_4O_{11}$ (*4*) are distributed between a pair of adjacent 4*f* positions. These Fe ions, however, have a coordination sphere intermediate between trigonal-bipyramids and tetrahedra, while Fe(3) ions in $SrFeV_5O_{11}$ have almost distortion-free tetrahedral coordination spheres. Actually, both the Fe(3)–O(2) and the

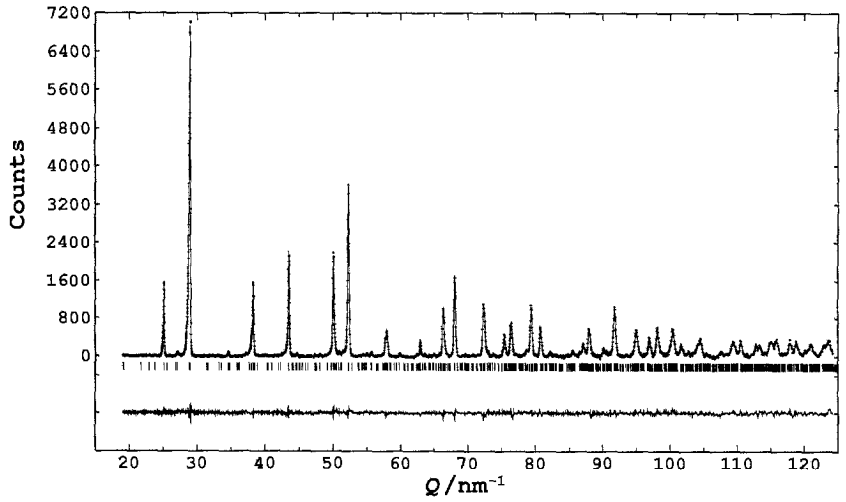

FIG. 3. The observed (+ marks), calculated (upper solid line), and difference (lower solid line) neutron powder diffraction profiles of $SrCrV_5O_{11}$. The background has been subtracted to show net intensities. Reflection positions are indicated by vertical bars.

TABLE VII

LATTICE PARAMETERS (Å), OCCUPANCIES(g) OF $T(n)$, AND INTERATOMIC DISTANCES (Å) IN $SrT_xV_{6-x}O_{11}$

Parameter		$SrTiV_5O_{11}$	$SrTi_{1.5}V_{4.5}O_{11}$	$SrCrV_5O_{11}$	$SrFeV_5O_{11}$	SrV_6O_{11}[a]
a		5.7844(1)	5.7980(2)	5.7706(2)	5.7592(1)	5.7716(1)
c		13.2103(3)	13.2271(3)	13.0607(3)	13.2170(2)	13.0793(5)
$g(T(1))$		0.12(2)	0.13(2)	0.15(1)	0	
$g(T(2))$		0.24(3)	0.39(3)	0.23(2)	0.238(4)	
$g(T(3))$		0.16(7)	0.35(9)	0.07(6)	0.564(8)	
$M(1)$—$O(1^{i})$	(×4)	1.967(2)	1.965(4)	1.948(2)	1.975(2)	1.945(3)
$M(1)$—$O(3^{ii})$	(×2)	2.052(2)	2.049(5)	2.050(2)	2.051(2)	2.029(6)
mean $M(1)$—O		1.995	1.993	1.982	2.000	1.973
$M(2)$—O(1)	(×3)	1.919(7)	1.927(9)	1.92(2)	1.876(5)	1.949(2)
$M(2)$—$O(2^{ii})$	(×3)	2.076(5)	2.067(7)	2.08(1)	2.107(4)	2.026(1)
mean $M(2)$—O		1.998	1.997	2.00	1.992	1.988
$M(3)$—O(2)	(×3)	1.808(4)	1.818(6)	1.787(4)	1.802(3)[b]	1.832(6)
	(×3)				1.817(4)[c]	
$M(3)$—$O(3^{iii,iv})$	(×2)	2.110(4)	2.124(8)	2.071(4)	2.103(4)[b]	2.11(1)
	(×1)				1.867(9)[c]	
	(×1)				2.339(9)[c]	
Sr—O(1)	(×6)	2.730(3)	2.754(6)	2.718(4)	2.714(2)	2.697(3)
Sr—$O(2^{ii})$	(×6)	2.8955(2)	2.9026(3)	2.8878(2)	2.8830(2)	2.891(4)
mean Sr—O		2.813	2.828	2.803	2.799	2.794
$M(2)$—$M(2^{v})$		2.80(3)	2.78(3)	2.77(9)	2.91(2)	2.721(3)
$M(2)$—$M(2^{vi})$		3.80(3)	3.83(3)	3.76(9)	3.70(2)	3.819(7)
$M(3)$—$M(3^{iv})$		0	0	0	0[b]	0
					0.47(1)[c]	

Note. Symmetry codes: (i) $1 - y, x, z$; (ii) $y, x, z - 1/2$; (iii) x, y, z; (iv) $x, y, 3/2 - z$; (v) $x, y, 1/2 - z$; (vi) $x, y, -z$.

[a] From Ref (*3*).

[b] V—O or V—V distance.

[c] Fe—O or Fe—Fe distance.

shorter Fe(3)–$O(3^{iii,iv})$ bond lengths in $SrFeV_5O_{11}$ (Table VII) are nearly equal to the sum of ionic radii, $r(^{IV}Fe^{3+}) + r(^{IV}O^{2-})$ = 1.87 Å (*16*), where roman numerals denote coordination numbers. The lattice parameter a of $SrFe_xV_{6-x}O_{11}$ decreases with increasing x (see Fig. 2), which indicates that the average O(2)–O(2) distance decreases with increasing occupancy of Fe in the $M(3)$ site. The edge of the basal plane for an FeO_4 tetrahedron is shorter than that for a VO_5 trigonal bipyramid.

Differences in the lattice parameters c and the $M(2)$–$M(2^{v})$ distances among SrV_6O_{11}, NaV_6O_{11} (*3*), $BaTi_2Fe_4O_{11}$, and $BaSn_2Fe_4O_{11}$ (*4*) are attributed merely to the deviations of the $M(3)$ sites from the ideal $2d$ position (*3*). This discussion is inapplicable to $SrFeV_5O_{11}$ having the split Fe(3) site, because the $O(3^{iii})$–$O(3^{iv})$ bond in $SrFeV_5O_{11}$

is not longer than that in SrV_6O_{11} having the unsplit V(3) site (Table VII).

In $BaTi_2Fe_4O_{11}$ and $BaSn_2Fe_4O_{11}$, the results of Madelung energy calculations (*3*) were consistent with the experimental results (*4*) that the $M(3)$ sites are occupied by Fe^{3+} exclusively. However, the present calculations for $SrFeV_5O_{11}$ (Table VIII) indicated that the $M(3)$ site ($4f$) is preferred by tetravalent cations, which is in conflict with the experimental result that this site is occupied by Fe^{3+}. This is probably due to the relatively large deviations of the $M(3)$ site ($4f$) from the ideal $2d$ position in $SrFeV_5O_{11}$. The above results suggest a strong preference for the tetrahedral site by Fe^{3+}.

(*b*) *$SrCrV_5O_{11}$*. Though the Madelung energy calculation suggests that the $M(3)$ site tends to accommodate a trivalent cation, the occupation factor of Cr^{3+} at this site is minimal (Table VII). This result is consistent with a very strong preference for the octahedral site by Cr^{3+} having a $3d^3$ electron configuration. A crystal field stabilization energy for this electron configuration in trigonal-bipyramidal coordination, $(25/4)D_q$ (*17*), is indeed much smaller than that, $12D_q$, for the same electron configuration in octahedral cordination.

(*c*) *$SrTiV_5O_{11}$ and $SrTi_{1.5}V_{4.5}O_{11}$*. Contrary to the prediction from the Madelung energy calculations, about one-third of the $M(3)$ sites in $SrTi_{1.5}V_{4.5}O_{11}$ are occupied by Ti^{4+}, which suggests that Ti^{4+} prefers a five-coordinated site while V^{3+} does not. Indeed, five-coordinated Ti^{4+} has been found in, for example, Y_2TiO_5 (*18*), K_2TiO_5 (*19*), and $Ba_2TiSi_2O_8$ (*20*), while no examples of five-coordinated V^{3+} are compiled in the literature (*16*).

It is, however, worth noting that at least 15% of the $M(3)$ sites must be occupied by V^{3+} because there is only 0.5 V^{4+} in the formula unit, which is not sufficient to occupy the rest of the $M(3)$ sites.

(*d*) *General remarks*. Both the $M(1)$ and the $M(2)$ sites are octahedrally surrounded by six O atoms, and there is no significant difference between the mean $M(1)$–O and mean $M(2)$–O distances. However, V(1)

TABLE VIII

ELECTROSTATICALLY MOST STABLE CHARGE DISTRIBUTIONS IN THE $M(1)$, $M(2)$, AND $M(3)$ SITES, THEIR ELECTROSTATIC SITE POTENTIALS (ϕ), AND MADELUNG ENERGIES (ΔE) IN $SrT_xV_{6-x}O_{11}$ COMPOUNDS

	$SrTiV_5O_{11}$	$SrTi_{1.5}V_{4.5}O_{11}$	$SrCrV_5O_{11}$	$SrFeV_5O_{11}$[a]	$SrFeV_5O_{11}$[b]	SrV_6O_{11}
$M(1)$	+3	+3	+3	+3	+3	+3
$M(2)$	+4	+4	+4	+4	+3[c] +4[d]	+4
$M(3)$	+3	+3	+3	+3	+4	+3
$\phi(M(1))$ (V)	−35.17	−35.48	−35.57	−34.37	−34.70	−36.01
$\phi(M(2))$ (V)	−43.13	−43.12	−42.98	−43.78	−37.10[c] −44.44[d]	−42.96
$\phi(M(3))$ (V)	−37.74	−37.20	−38.39	−38.37	−44.48	−36.91
ΔE (MJ · mol^{-1})	−5.469	−5.467	−5.496	−5.480	−5.489	−5.492

[a] All the $M(3)$ atoms are assumed to be at the $2d$ position.

[b] All the $M(3)$ atoms are assumed to be at a $4f$ position. That is, cations are distributed between a pair of adjacent positions, (1/3, 2/3, 3/4 ± Δz). For the calculation of the Madelung energy, however, the $M(3)$ atoms were approximated to occupy one of the paired positions according to the space group $P6_3mc$. Consequently, the $M(2)$ site closer to the neighboring $M(3)$ atom and the remaining one are not equivalent.

[c] Closer to the neighboring $M(3)$ atom.

[d] More distant from the neighboring $M(3)$ atom.

ions are generally less replaced by T ions. Actually, g(Cr(1)) is smaller than g(Cr(2)) in $SrCrV_5O_{11}$ contrary to the Madelung energy calculations. In particular, Fe ions cannot enter into the $M(1)$ site. The reason for this tendency remains unknown as yet.

De Roy *et al.* (*1*) selected $P\bar{6}2c$ symmetry for NaV_6O_{11} from three possible space groups, $P6_3/mmc$, $P\bar{6}c$ and $P6_3mc$, because only the $P\bar{6}2c$ space group gave reasonable Na–O distances. However, our structure refinements (*3*) showed that SrV_6O_{11} and NaV_6O_{11} crystallize in $P6_3/mmc$ rather than $P\bar{6}c$. The present structural refinements based on $P6_3/mmc$ also gave the reasonable Sr–O distances consistent with $r(^{XII}Sr^{2+}) + r(^{IV}O^{2-}) = 2.82$ Å (*16*).

References

1. M. E. DE ROY, J. P. BESSE, R. CHEVALIER, AND M. GASPERIN, *J. Solid State Chem.* **67,** 185 (1987).
2. Y. KANKE, E. TAKAYAMA-MUROMACHI, K. KATO, AND Y. MATSUI, *J. Solid State Chem.* **89,** 130 (1990).
3. Y. KANKE, K. KATO, E. TAKAYAMA-MUROMACHI, AND M. ISOBE, *Acta Crystallogr., Sec. C,* submitted for publication.
4. M. C. CADÉE AND D. J. W. IJDO, *J. Solid State Chem.* **52,** 302 (1984).
5. W. D. TOWNES, J. H. FANG, AND A. J. PERROTTA, *Z. Kristallogr.* **125,** S.437 (1967).
6. P. B. BRAUN, *Philips Res. Rep.* **12,** 491 (1957).
7. E. KNELLER, M. VELICESCU, AND F. HABEREY, *J. Magn. Magn. Mater.* **7,** 49 (1978).
8. R. S. TEBBLE AND D. J. CRAIK, "Magnetic Materials," Chap. 10, pp. 362–363, John Wiley, New York (1969).
9. J. S. VAN WIERINGEN, *Philips Tech. Rev.* **28,** 33 (1967).
10. R. L. STREEVER, *Phys. Rev.* **186,** 285 (1969).
11. N. WATANABE, H. ASANO, H. IWASA, S. SATOH, H. MURATA, K. KARAHASHI, S. TOMOYOSHI, F. IZUMI, AND K. INOUE, *Jpn. J. Appl. Phys.* **26,** 1164 (1987).
12. F. IZUMI, H. ASANO, H. MURATA, AND N. WATANABE, *J. Appl. Crystallogr.* **20,** 411 (1987).
13. V. F. SEARS, "Neutron Scattering, Part A. Methods of Experimental Physics," Vol. 23. (K. Sköld and D. L. Price, Eds.) Vol. 23, p. 521, Academic Press, New York (1986).
14. L. KOESTER, H. RAUCH, M. HERKENS, AND K. SCHRÖDER, "Summary of Neutron Scattering Lengths," KFA-Report, Jül-1755 (1981).
15. JCPDS CARD, NO. 35-734 (1985).
16. R. D. SHANNON, *Acta Crystallogr., Sec. A* **32,** 751 (1976).
17. J. S. WOOD, "Progress in Inorganic Chemistry," (S. J. Lippard, Ed.), Vol. 16, p. 295, Wiley, New York (1972).
18. W. G. MUMME AND A. D. WADSLEY, *Acta Crystallogr. Sec. B* **24,** 1327 (1968).
19. S. ANDERSSON AND A. D. WADSLEY, *Acta Chem. Scand.* **15,** 663 (1961).
20. P. B. MOORE AND J. LOUISNATHAN, *Science* **156,** 1361 (1967).